

# FRP – CONCRETE DELAMINATION RESULTS ADOPTING DIFFERENT EXPERIMENTAL PURE SHEAR SETUPS

C. Mazzotti, M. Savoia and B. Ferracuti  
DISTART - Structural Engineering, University of Bologna, Bologna, Italy

## ABSTRACT

A new experimental setup for FRP – concrete delamination is described. Four specimens with different bond lengths have been tested. Starting from experimental data, a non linear interface law has been calibrated. Making use of a bond – slip model, numerical results are obtained, in good agreement with experimental results. Comparison with results obtained from traditional setups for pure shear tests are performed.

## 1 INTRODUCTION

In order to define the bearing capacity of FRP strengthened r.c. beams, delamination problem must be carefully taken into account. Delamination may arise from extremities of reinforcement (end debonding) or from intermediate cracks in the concrete (Teng [1], Leung [2]). In both cases, it is due to the lower strength of interface under mode II condition with respect to two principal materials, concrete and reinforcing composite. Very few experimental studies can be found in literature which can be useful to calibrate a FRP – concrete interface law. Most of them adopt a “standard” delamination experimental setup where FRP plate is bonded at one end of a concrete specimen (Täljsten [3], Mazzotti [4]). In these tests, failure mechanism is affected by a boundary effect due to concrete spalling in the traction side of the specimen, when delamination occurs.

The results of an experimental campaign on FRP–concrete delamination using a non standard setup are presented in this paper. Plates have been glued far from the specimen front side. Then, starting from experimental data, a non linear interface law has been calibrated.

A bond – slip model, originally presented in Savoia [5], has been used to simulate experimental tests. Numerical results are found to be in good agreement with experimental results.

Finally, comparison between experimental results obtained from the present setup and the standard setup for pure shear delamination tests are compared. The proposed setup appears to be more appropriate to obtain data for the calibration of a local interface bond-slip law.

## 2 GEOMETRY AND MECHANICAL PROPERTIES OF SPECIMENS

Four specimens have been realized by glueing CFRP plates of different lengths (50, 100, 200, 400 mm) to concrete blocks. Mechanical and geometrical properties of concrete blocks (150×200×600 mm) and composite plates are summarized in Table 1.

Top surfaces of concrete blocks have been grinded with a stone wheel to remove the top layer of mortar, just until the aggregate was visible (approximately 1 mm). Plates have been bonded to the top surface of blocks by using a 1.5 mm thick layer of two – components epoxy adhesive Sikadur-30. Plate bonded length has been positioned 100 mm from the front side of the concrete specimen.

## 3 EXPERIMENTAL SETUP

The concrete blocks were positioned on a rigid frame with two steel reaction elements to prevent horizontal and vertical translations (Figure 1); the free end of the plate was clamped to a steel plate that was free to rotate around the vertical axis.

Concrete		CFRP plates	Sika CarboDur S
$f_{cm}$ [MPa]	52.6	Width [mm]	50
$f_{ctm}$ [MPa]	3.81	Thickness [mm]	1.2
$E_{cm}$ [MPa]	30700	$f_{ptm}$ [MPa]	2200
$\nu$	0.227	$E_p$ [MPa]	165000

Table 1: Mechanical and geometrical properties of concrete and CFRP plates.

The traction force was applied to the steel plate by using a mechanical actuator. Tests were performed under displacement control of the plate free end. A load cell has been used to record the applied traction force. Along the CFRP plate, a series of five–to–nine strain gauges (depending on the plate length) were placed, in the centerline. Moreover, two LVDTs were placed in order to measure displacements (Figure 1): at the beginning of the bonded length and in the lower portion of the front side of the concrete block, so that relative displacements can be computed.

#### 4 RESULTS OF DELAMINATION TESTS

##### 4.1 Experimental results

For the four different bonded lengths, longitudinal strains along the FRP plate at different loading levels are reported in Figure 2. The corresponding values of applied force are reported in Table 2. The strain at  $x = 0$  corresponds to that calculated from the value of external applied force.

For bonded lengths from 100 mm to 400 mm, FRP strains are very regular for low – to – medium values of applied force, showing an exponential decay from the loaded section ( $x = 0$ ). This strain profile corresponds to a linear behavior of the interface. For high force levels, strains tend to be almost constant along FRP plate close to loaded end, due to onset of delamination phenomenon along the bonded length; in the portion of specimens which is not delaminated, an exponential decay behavior of strains can be observed again. On the contrary, for the 50 mm bonded length, strain profiles are almost linear along the bonding length, indicating a uniform distribution of shear stresses. The result confirms that the shortest bond length is significantly smaller than the effective anchorage length (the minimum length assuring maximum FRP anchoring force), and non–vanishing slip occurs along the whole specimen.

The experimental values of maximum forces at failure as a function of bonded length are reported in Figure 3(a). In all specimens, failure was caused by shearing of a layer of concrete about 1-2 mm thick. An interpolation curve is also reported, which has been used to predict the value of maximum transmissible force by an anchorage of infinite length, which is then estimated equal to about  $F_{max} = 23$  kN.

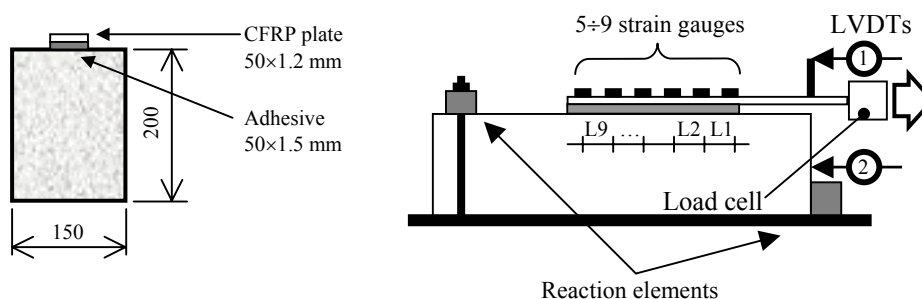


Figure 1: Geometry of FRP – concrete specimens and scheme for delamination tests.

Bond Length	F1	F2	F3	F4	F5	F6	F7	F8	F9	F10	F11
50	4.0	8.0	10.0	12.0	13.0	14.0					
100	4.0	8.0	10.0	12.0	16.0	18.0	20.0	22.0	22.3		
200	4.0	8.0	10.0	12.0	16.0	18.0	19.8	19.0	18.0		
400	4.0	8.0	12.0	16.0	20.0	22	23.0	21.0	20.0	19.0	18.0

Table 2: Levels of applied force (kN) corresponding to FRP – strain profiles in Figure 2.

For the calibration of interface law, a two-step procedure is adopted, originally proposed in [4], where the reader is addressed for additional details.

First of all, it has been shown in Mazzotti [4] that the following relation between maximum transmissible force  $F_{\max}$  and fracture energy  $G_f$  of interface law:

$$F_{\max} = b_p \sqrt{2E_p h_p G_f}, \quad (1)$$

holds for every mode II interface law (neglecting concrete compliance), where  $E_p$ ,  $h_p$ ,  $b_p$  are elastic modulus, thickness and width of the plate, respectively. The relation (1) is valid for every interface law expressed by a sufficiently regular function.

Eqn (1) is used to calculate the fracture energy of interface law, obtaining the value  $G_f = 0.525$  kN/mm.

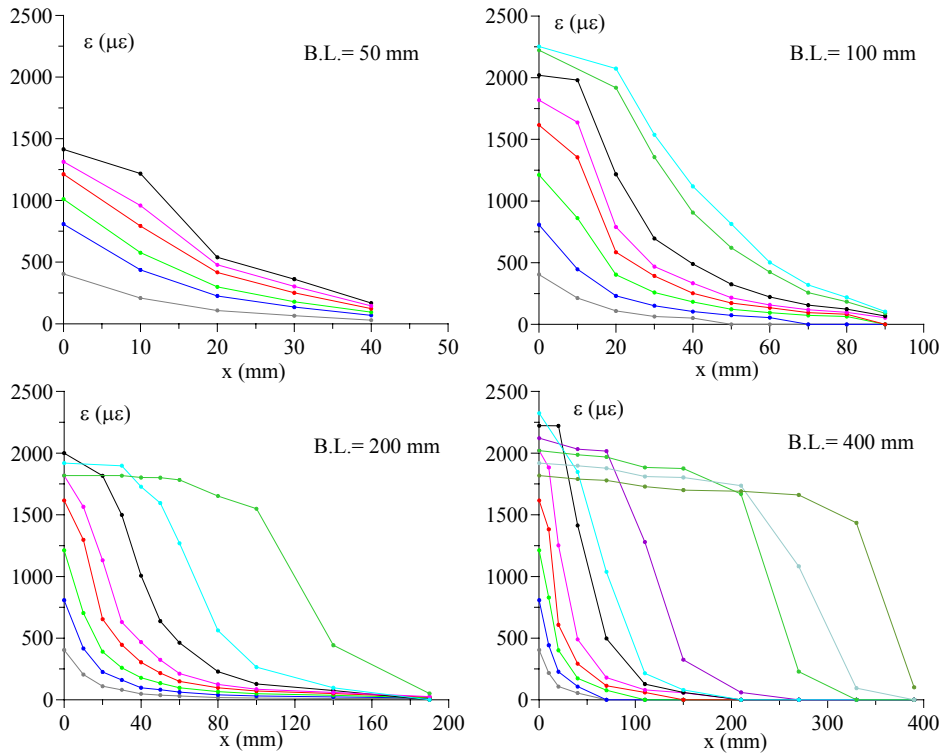


Figure 2: Profiles of experimental strains in FRP plates along the bonded lengths. Level loads are reported in Table 2.

As a second step, experimental strains along the FRP plate have been post-processed, in order to calculate shear stress and slip distributions along the bonded lengths. Denoting by  $x_i$  the strain gauge position and  $\varepsilon_i$  the corresponding measured strain, the average value of shear stress between two subsequent strain gauges can be written as

$$\bar{\tau}_{i+1/2} = \frac{E_p A_p (\varepsilon_{i+1} - \varepsilon_i)}{b_p (x_{i+1} - x_i)}, \quad (2)$$

with  $A_p$  being cross section of the composite. Moreover, assuming, for the sake of simplicity, perfect bonding (no slip) at last strain gauge position and neglecting concrete strain with respect to FRP counterpart, integration of strain profile gives the following expression for the slip at  $x$ , with  $x_i \leq x \leq x_{i+1}$ :

$$s(x) = s(x_i) + \int_0^x \varepsilon(x) dx = s(x_i) + \frac{(\varepsilon_{i+1} - \varepsilon_i) x^2}{(x_{i+1} - x_i) 2} + \varepsilon_i x. \quad (3)$$

Eqn (3) is used to compute the average slip between the two positions  $x_i, x_{i+1}$ , denoted by  $\bar{s}_{i+1/2}$ . When computing shear stresses and slips, some irregular values in FRP strain profiles for high loadings have been removed. For the four bonded lengths, shear stress – slip data obtained from experimentally measured FRP-strains are shown in Figure 3(b).

For the shear stress – slip interface law, a Popovics' type formula is adopted:

$$\tau_p = \bar{\tau} \frac{s_p}{\bar{s}} \frac{n}{(n-1) + (s_p / \bar{s})^n}, \quad (4)$$

where  $(\bar{\tau}, \bar{s})$  denotes the maximum shear stress and corresponding slip, and  $n$  is a free parameter. The three unknown parameters have been identified by using a mean square fitting procedure with respect to experimental data reported in Figure 3(b), where the value of fracture energy previously obtained has been used as a constraint in the minimization procedure. The values  $\bar{\tau} = 9.141$  MPa,  $\bar{s} = 0.0334$  mm,  $n = 4.188$  have been obtained. In Figure 3(b), the interface law is compared with experimental data.

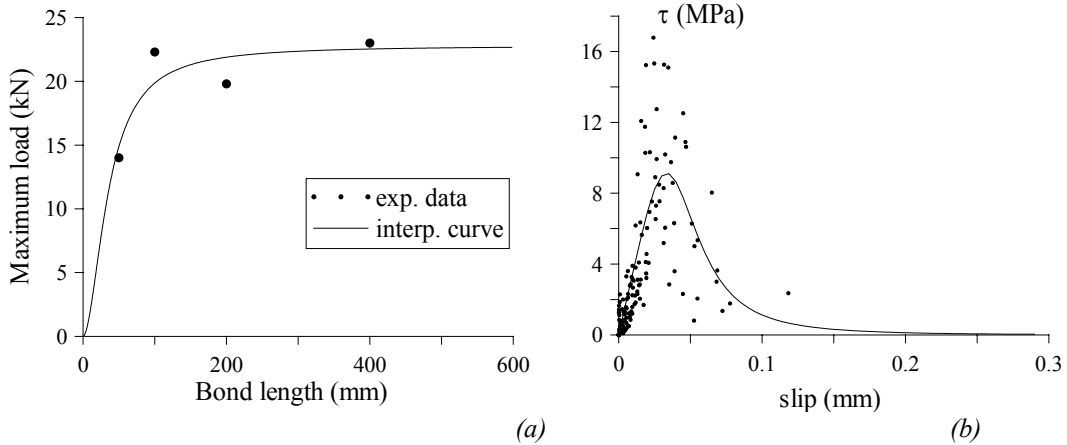


Figure 3: (a) Delamination load as a function of bond length: experimental results and interpolation curve; (b) Shear stress – slip experimental data and the proposed non linear interface law.

## 5 NUMERICAL SIMULATION OF EXPERIMENTAL TESTS

Experimental tests have been numerically simulated making use of the numerical model recently proposed by the Authors [5]. Linear elastic behavior is assumed for concrete and FRP-plates, whereas the non linear law reported in Figure 3(b) is used for the interface.

For the bonded length  $L=400$  mm, comparison between experimental and numerical strain distribution is reported in Figure 4(a), whereas shear stresses are compared in Figure 4(b). It is worth noting that the numerical model predicts well experimental bond behaviour both during loading increase (low stress level) and during delamination process. In the second case, diagrams refer to equilibrium condition after the attainment of maximum load. Analogously, note the shear stress distributions reported in Figure 4(b): the translation of the portion of interface transferring shear stresses from the loaded (left) to the end (right) section of the anchorage is well predicted by numerical simulation.

## 6 COMPARISON BETWEEN RESULTS FROM DIFFERENT EXPERIMENTAL SETUP

The experimental setup described in the present paper is a modified version of the usual setup for delamination tests under mode II condition, where the bonding length ends at the front side of the concrete specimen (called setup 1). The authors recently performed delamination tests with identical materials as described here but adopting setup 1. Instead, in the tests presented here the bonded length starts 100 mm far from the front side of the specimen (called setup 2), see Figure 2. The strain distributions obtained for  $L = 400$  mm with the two setups are reported in Figure 5. Same colors refer to the same loading level. Note that in the first case (Figure 5 (a)) decay of axial strains along the bonding length adopting setup 2 is always higher than with setup 1. This behavior denotes higher stiffness of the interface in the case of setup 2. Analogously, after the attainment of maximum load (Figure 5(b)) softening behaviour adopting setup 1 is much more brittle and a limited portion only of bonded length is involved in the plate delamination process (no more than 250 mm) before complete failure; on the contrary, adopting setup 2 a stable and complete delamination process can be observed.

The different behavior has an interesting mechanical explanation: with setup 1, i.e. when bonding length starts at the front side of the specimen, the first portion of the specimen is subject to traction stresses which are not equilibrated (see Figure 6(a)). Since the length of that portion is comparable with the transmission length of the interface, its stiffness is lower than in setup 2 and

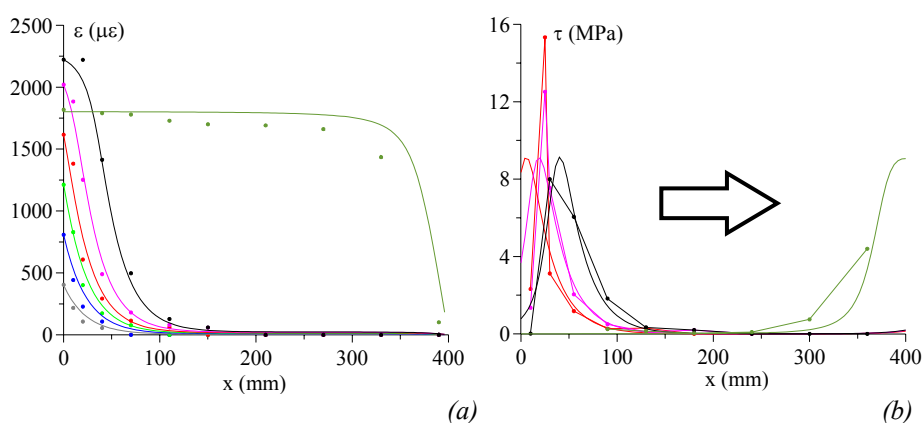


Figure 4: Comparison between experimental data and numerical results: (a) Profiles of strains in FRP plates and (b) shear stresses along the bonded lengths.

failure is more brittle. On the contrary, adopting setup 2 no boundary effects occur and delamination area is very regular (see Figure 6(b)). The same behaviour has been observed for all bonded lengths considered in experimental tests. For these reasons, setup 2 is considered more appropriate to obtain data for the calibration of a local interface bond-slip law.

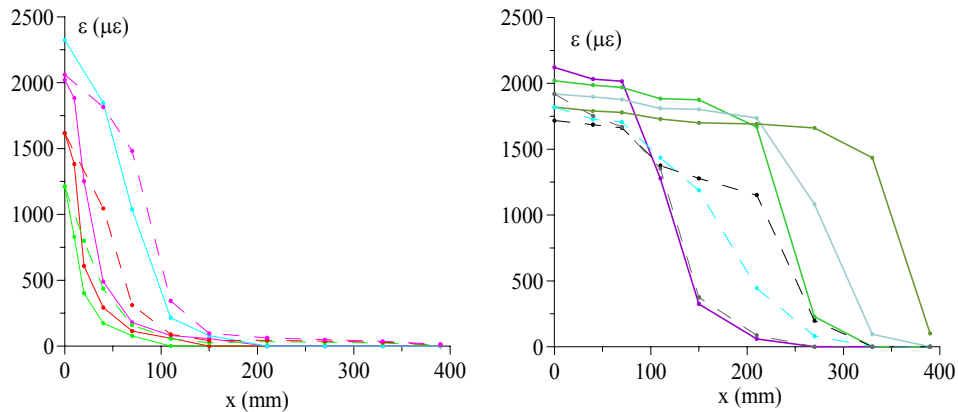


Figure 5: Comparison between experimental data of FRP- strains (a) at load levels lower than maximum load, (b) during unloading after delamination: (---) setup 1, (—) setup 2.

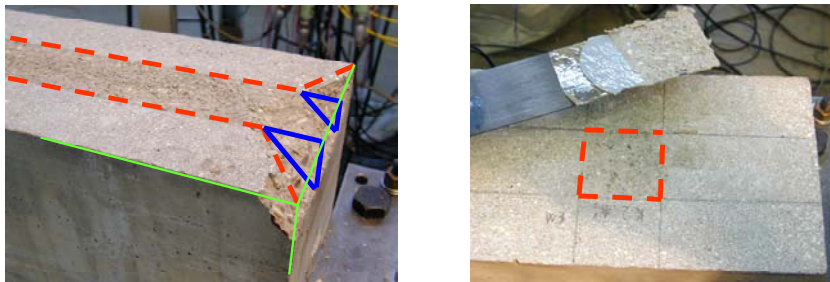


Figure 6: Specimens tested according to (a) setup 1 and (b) setup 2 after delamination.

#### ACKNOWLEDGEMENTS

The authors would like to thank the Sika Italia S.p.a. for providing CFRP plates and adhesives for the specimens. The financial supports of (italian) MIUR (PRIN 2003 Grant, FIRB Grant) and C.N.R., PAAS Grant 2001 are gratefully acknowledged.

#### REFERENCES

- [1] Teng J.G., Chen J.F., Smith S.T. & Lam L. *FRP strengthened RC structures*. J. Wiley and sons, UK, 2002.
- [2] Leung K.C.Y. Fracture mechanics of debonding failure in FRP-strengthened concrete beams. In Li et al. (ed.), *Proc. FraMCoS, Vail USA*, Vol. 1: 41-52, 2004.
- [3] Täljsten B. *Plate bonding* (doctoral thesis). Division of Structural Engineering, Luleå University, Sweden, 1994.
- [4] Mazzotti, C., Ferracuti B. & Savoia M. An experimental study on FRP –concrete delamination. In Li et al. (ed.), *Proc. FraMCoS, Vail USA*, Vol. 2: 795-802, 2004.
- [5] Savoia, M., Ferracuti B. & Mazzotti C. (2003). Delamination of FRP plate/sheets used for strengthening of R/C elements. In F. Bontempi (ed.), *ISEC-02*, Balkema, Vol. 2: 1375-1361.